

International Congress on Ultrasonics, Universidad de Santiago de Chile, January 2009

Sonoelectrochemical synthesis of magnetite

L. Cabrera^{a,b}, S. Gutiérrez^b, P. Herrasti^a, D. Reyman^{a*}

^a *Facultad de Ciencias, Universidad Autónoma de Madrid, Cantoblanco s/n 28049 Madrid*

^b *IIC, Universidad de Guanajuato, Cerro de la Venedad s/n 36040 Guanajuato*

Abstract

The effects of ultrasound (US) on the direct electrosynthesis of magnetite (Fe₃O₄) nanoparticles are investigated. The electrochemical system consists of two electrodes; anode and cathode, both of iron, and 99.5% purity. The anode is a sacrificial electrode, which when oxidized generates the desired Fe₃O₄. Cationic surfactants are used in the synthetic system as supporting electrolytes and as a protective layer which covers the obtained nanoparticles in order to avoid aggregation.

In order to study the influence of ultrasound in the synthesis of Fe₃O₄, the experiments were compared to the same systems without the application of ultrasound.

Physical properties of the reaction product, such as morphology and particle size, were characterized by means of X-ray diffraction, and transmission electron microscopy. Size distribution studies in function of the application and variation of the US parameters are shown.

The effect of US on the magnetic properties of Fe₃O₄ was studied by means of hysteresis loops. The experimental results were compared to those obtained during the synthesis of Fe₃O₄ without the US presence.

Keywords: Magnetite; sonoelectrosynthesis; ultrasound

1. Introduction

Magnetite (Fe₃O₄) has many important applications, including magnetic storage media, solar energy transformation, electronics and catalysis. In general, the synthesis of Fe₃O₄ nanoparticles has been carried out by coprecipitation [1]. This method consists in mixing ferric and ferrous ions in a 1:2 molar ratio in highly basic solutions. In order to obtain well dispersed NP, surfactants such as dextran or polyvinyl alcohol can be added in the reaction media, or the particles can be coated in a subsequent step [2, 3]. However, this method generates wastewaters with very basic pH values, which require subsequent treatments.

The use of ultrasonic techniques has been studied thoroughly by Vijayakumar *et al.* for the generation of amorphous iron oxide materials [4]. Sonochemical synthesis has been used to prepare aggregated maghemite (γ -Fe₂O₃) nanoparticles of *ca.* 25 nm with octadecyltrihydrosilane (OTHS, CH₃(CH₂)₁₇SiH₃) in heptane from a solution

* Corresponding author. Tel.: 0-34-914978657; fax: 0-34-914974512.

E-mail address: dolores.reyman@uam.es

of Fe(CO)₅ in anhydrous decane [5]. Recently, Mancier *et al.* have produced by ultrasound-assisted electrochemistry nanopowders of several metals and alloys [6].

The latter system appears to be very attractive, since a number of possible effects of ultrasound (US) upon an electrochemical system may be predicted:

- a) A general improvement of hydrodynamics and movement of species.
- b) The alteration of concentration gradients at various points in the reaction profile, and consequent switching of kinetic regimes with effect on mechanism and reaction products.
- c) A cleaning and abrading effect upon an electrode surface, thus obviating fouling problems, or else altering the nature of coatings that manage to form.
- d) Sonochemical induced reactions of intermediate species that have been generated electrochemically.
- e) The sonochemical formation of species that react electrochemically in conditions where the silent system is electroinactive.

In sonochemistry, the acoustic cavitation, that is, the formation, growth, and implosive collapse of a bubble in an irradiated liquid, generates a transient localized hot spot, with an effective temperature of 5000 K of nanosecond lifetime, allowing mixing of the constituent species in the amorphous phase at an atomic level [5, 7-10]. The reason for obtaining amorphous nanoparticles, is the large cooling rates (in excess of 10^{11} K s⁻¹) obtained when the bubble collapses [4, 10].

In addition to these, chemical reactions are also induced by the cavitation phenomenon both inside the collapsing bubbles and in the liquid medium. Solvent and solute molecules present within the cavitation bubbles are decomposed and generate several highly reactive radicals. For example, if the sonicated medium is water, H[•] and OH[•] radicals are generated (1) [4, 9].



OH[•] radicals could react to give hydrogen peroxide, an oxidant that could initiate the oxidation of a metal ion such as Fe(II), (2) and (3)



Hence, Fe₃O₄ nanoparticles can be obtained using the ultrasound-electrochemical technique, where a sacrificial electrode can be the source of Fe(II).

In this work, we will study the effects of US over the electrochemical synthesis of Fe₃O₄, using an ultrasonic field of 24 kHz frequency.

2. Experimental

2.1. Synthesis

Two different synthetic systems were used, in order to compare the material generated in both cases.

In the first case, Fe₃O₄ was electrosynthesized in the absence of US. It was performed in a three mouth electrochemical cell. A sacrificial iron anode (2 cm² dimension, 0.2 mm thick) purchased from Goodfellow (purity 99.5%) and an iron cathode (8 cm²) was used for the synthesis. The electrodes were cleaned by sonication and ethanol before being used. The distance between both electrodes was optimized to obtain magnetite and kept at 1 cm for all experiments. The supporting electrolyte was 0.04 M, aqueous solution of Me₄NCl (Merck) salt. The water used was Milli-Q with an 18.2 MΩ resistance. The current density applied was kept constant, with $j = 100$ mA·cm⁻² by means of a potentiostat/galvanostat VesaStat™, EG&G Instruments Princeton Applied Research. Constant stirring was applied during the reaction. Reaction time was 1800 s in every case and the reaction temperature was

kept at 60°C with a thermostatic bath. The obtained product was washed with distilled water and dried for its subsequent characterization.

In the second case, the system employed was very similar, were the parameters studied and conditions established were the same, except that the electrochemical cell had an opening big enough to allow the introduction of an ultrasonic reactor (Hielscher Ultrasonic Processor, UP200S, 200 watts, 24 kHz), to sonicate the electrolytic solution during the reaction time. During all the reaction, the amplitude was adjusted to 35% and sonotrode, S14 (14 mm diameter) was used. The temperature (which reached values as high as 70°C) was measured during the reaction, but was not control with a water jacket.

2.2. Characterization methods

Particle size and shape were analyzed by transmission electron microscopy (TEM) in a JEOL-2000 FXII electron microscope operated at 200 keV. The mean particle size and distribution were calculated by measuring the internal dimension of at least 100 particles. The phase of the resulting iron oxide nanoparticles was investigated by X-ray diffraction. X-ray diffractograms were recorded between 10° and 100° 2θ in an X'Pet PRO Panalytical diffractometer, with θ -2θ geometry, equipped with a primary and secondary monochromators, and an ultrafast X'Celerator detector, with a CuK α radiation.

Magnetic characterization was carried out using a vibrating sample magnetometer (MLVSM9 MagLab 9T, Oxford Instrument). The magnetization curves were measured at room temperature after applying a maximum magnetic field of 1T. From the magnetization curves, the parameters of saturation magnetization (M_s) and coercitive field (H_c) were calculated.

3. Results and discussion

The first parameter studied, was the concentration of the supporting electrolyte solution, using concentrations of (a) 0.04, (b) 0.08 and (c) 0.12 M of Me $_4$ NCl. The curves E vs. time, when $j = 100 \text{ mA}\cdot\text{cm}^{-2}$ is applied with (Figure 1) and without (Figure 2) the presence of US were registered. As it can be observed in all cases, a constant value was reached after a time reaction around 900 s. It is also noticeable that as the molar concentration increases, the potential decreases, with (Figure 1) or without (Figure 2) applying US. It must be mentioned, that when the solution 0.12 M of Me $_4$ NCl was used without US, the curve shown (Figure 2.c) appears incomplete because the iron electrode employed was consumed. The experiences were repeated several times, without being able to reach the 1800 s reaction time.

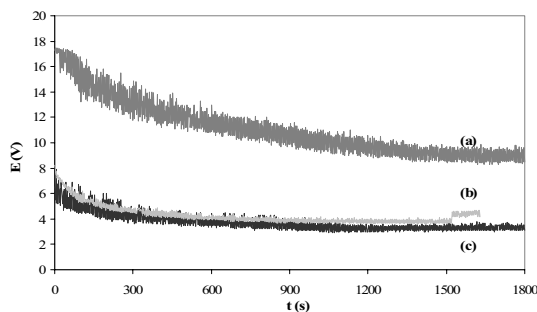


Fig.1 Electrolysis of Fe $_3$ O $_4$ applying US, E vs. t , $j = 100 \text{ mA}\cdot\text{cm}^{-2}$, electrolytic solution Me $_4$ NCl, a) 0.04 M; b) 0.08 M; and c) 0.12 M.

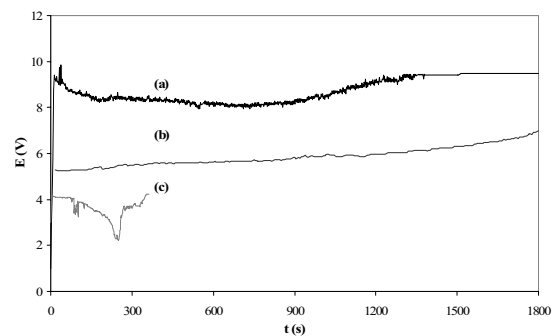


Fig. 2 Electrolysis of Fe $_3$ O $_4$ with constant stirring, $T = 60^\circ\text{C}$, E vs. t , $j = 100 \text{ mA}\cdot\text{cm}^{-2}$, electrolytic solution Me $_4$ NCl, a) 0.04 M; b) 0.08 M; and c) 0.12 M.

It is obvious that the solution resistance decreases as the electrolytic concentration is increased, allowing a better charge transfer between the electrodes. The use of US increases the ratio noise/signal, but it can not be denied that the tendency of the curve is better than in the absence of US. In the presence of US the potential achieved using Me_4NCl 0.08 and 0.12 M are practically the same, than in the absence of US. It is known, that during the oxidation of the iron electrode, two processes take place, charge transfer and iron ions diffusion into the electrolytic solution. It is possible, that when assisted by US, the oxidation of the sacrificial electrode has a better charge transfer than the other system, since the oxide layer that is formed at the surface of the iron electrode is being removed. Hence, the potential at the interface evidences the difference between both systems.

A black precipitate was obtained by electrooxidation under both conditions described in section 2.1. Characterization of the material was performed by X-ray diffraction. Figure 3 shows the diffractograms of the material obtained using 0.04 M Me_4NCl with and without US assistance.

All peaks have been indexed as the corresponding ones to magnetite (reference code: JCPDS 01-088-0315) and no impurities were present. The crystal size was calculated from the broadening of the (3 1 1) reflection of the spinel structure and the obtained values (23.5 nm and 22.8 nm for US assisted) were similar and within the margin error to the ones determined by TEM. Figure 4 shows TEM images of samples obtained with and without assistance of US respectively. The particles are quasi-spherical with a mean particles size for the former case of 22.4 nm and 23.8 nm for the latter one (US assisted). On the other hand, the maximum of the gaussian curve is at 23.6 nm without US and 26 nm with US, with a standard deviation of 4 nm and 7 nm respectively. The good agreement between crystal size by X-ray diffraction and particle size from TEM studies indicates the high crystalline character. On the other hand, histograms show (Figure 5 and 6) that particle size distribution becomes wider when assisted by US, probably due to the aggregation of the particles generated.

The aggregation phenomenon of the particles has been reported as a is intrinsic characteristic when US is employed, since the high velocity of interparticle collisions during the sonication causes the particles to collide [5]. This can be appreciated in the micrographs shown in Figure 4. Fe_3O_4 obtained in the absence of US appears more disperse than the ones obtained with the assistance of US. Such phenomenon could be also reflected in the magnetic properties of the material. Magnetic susceptibility is a property that is bound to the particle size, while coercivity could be related to the interactions between the Fe_3O_4 nanoparticles.

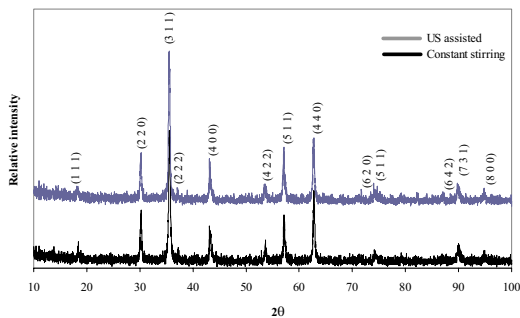


Fig.3 X-ray diffractograms of Fe_3O_4 generated electrochemically with and without the assistance of US.

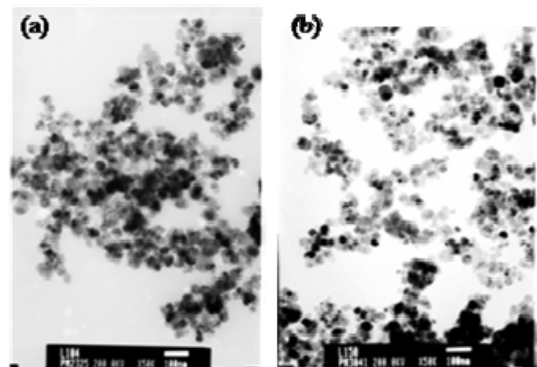


Fig.4 TEM micrographs obtained of Fe_3O_4 nanoparticles generated electrochemically (a) with and (b) without US assistance.

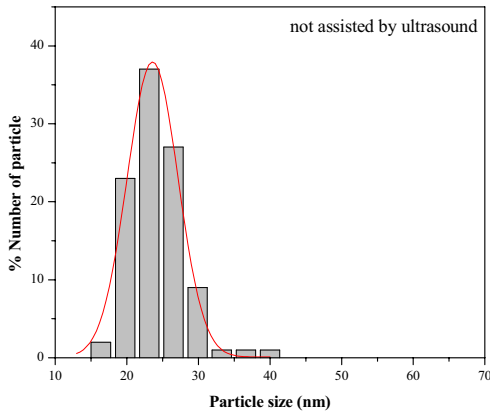


Fig.5 Size distribution histogram for Fe_3O_4 nanoparticles obtained without US assistance.

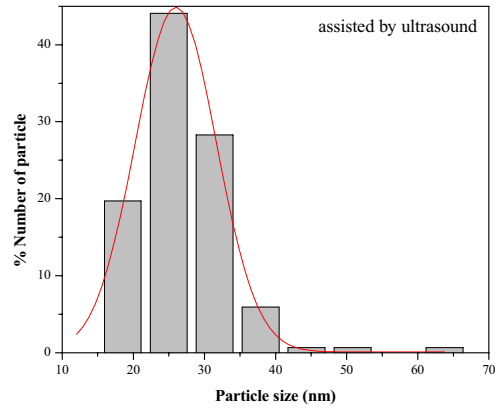


Fig.6 Size distribution histogram for Fe_3O_4 nanoparticles obtained with US assistance.

Figure 7 shows the magnetization curve recorded for Fe_3O_4 nanoparticles at RT. Ferromagnetic behavior was observed in both cases with a hysteresis loop typical of magnetite nanoparticles with sizes larger than 10 nm. The lack of magnetization at high fields is a well-known effect due to the small particle size and the high surface area, which lead to some spin canting. For Fe_3O_4 obtained in the absence of US, the saturation magnetization (M_s) was of $70 \text{ emu}\cdot\text{g}^{-1}$ and the coercivity (H_c) of 142 Oe. The M_s value is slightly lower than the reported value for bulk Fe_3O_4 ($92 \text{ emu}\cdot\text{g}^{-1}$ at RT), which can be referred to surface effects, i.e., spin canting. However, the coercivity is in agreement with the expected value for random oriented, uniaxial and non-interacting particles of magnetite.

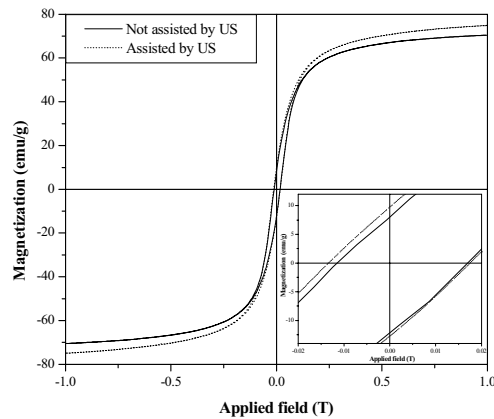


Fig.7 Magnetization curve at RT for Fe_3O_4 nanoparticles obtained with and without US assistance.

When the electrosynthesis of Fe_3O_4 is US-assisted, the value of H_c is higher than the former one ($H_c = 155 \text{ Oe}$). Even when the size of the particle is slightly bigger than the first case, it is most likely that the increase in H_c is due to the aggregation phenomenon, where the nanoparticles are not behaving as such, but as agglomerates. The saturation magnetization (M_s) was of $74 \text{ emu}\cdot\text{g}^{-1}$, higher than in the former case. Normally, when the

electrosynthesis of Fe_3O_4 is performed without US-assistance, a dead-oxide layer of Fe_2O_3 surrounds the Fe_3O_4 nanoparticle, decreasing its M_s [11], showing spin canting effects. US cleans the surface of the nanoparticle, eliminating the dead oxide layer, promoting the increase in M_s . However, it is also possible that, due to the increase in size, the number of domains is higher in the Fe_3O_4 nanoparticles electrosynthesized with US assistance than in the absence of it, giving a higher value in M_s [11]. Other explanations involving noncollinear spins can be also plausible. It has been previously reported that the difference may rely on the existence of noncollinear spins at the surface of the nanoparticle of Fe_3O_4 obtained without using US [11].

4. Conclusion

The electrochemical synthesis assisted by US, affords nanoparticles which form aggregates. The size distribution is affected by this phenomenon, as are affected the magnetic properties, where Fe_3O_4 generated with the assistance of US has higher H_c (155 Oe) and M_s ($74 \text{ emu}\cdot\text{g}^{-1}$) values than when generated in the absence of US ($H_c = 142 \text{ Oe}$; $M_s = 70 \text{ emu}\cdot\text{g}^{-1}$).

Acknowledgments

We gratefully acknowledge the support received from the DGICYT (Spain) (Project I+D: CTQ2005-04469) for this research.

References

- [1] V.L. Calero Díaz del Castillo, Master of Science, University of Puerto Rico, 2005
- [2] A.A. Novakova, V.Y. Lanchinskaya, A.V. Volkov, T.S. Gendler, T.Y. Kiseleva, M.A. Moskvina, S.B. Zezin. *J. Magn. Magn. Mater.*, vol. 258-259, pp. 354, 2003
- [3] P. Sipos. "Manufacturing of size controlled magnetite nanoparticles potentially suitable for the preparation of aqueous magnetite fluids," *Rom. Rep. Phys.*, vol. 58, pp. 269-272, 2006
- [4] R. Vijayakumar, Y. Koltypin, I. Felner, A. Gedanken. "Sonochemical synthesis and characterization of pure nanometer-sized Fe_3O_4 particles," *Mater. Sci. Eng. A*, vol. 286, pp. 101-105, 2000
- [5] K.V.P.M. Shafi, A. Ulman, A. Dyal, X. Yan, N.-L. Yang, C. Estournès, L. Fournès, A. Wattiaux, H. White, M. Rafailovich. "Magnetic Enhancement of $\gamma\text{-Fe}_2\text{O}_3$ Nanoparticles by Sonochemical Coating," *Chem. Mater.*, vol. 14, pp. 1778-1787, 2002
- [6] V. Mancier, J.-L. Delplancke, J. Delwiche, M.-J. Hubin-Franskin, C. Piquer, L. Rebbouh, F. Grandjean. "Morphologic, magnetic, and Mössbauer spectral properties of $\text{Fe}_{75}\text{Co}_{25}$ nanoparticles prepared by ultrasound-assisted electrochemistry," *J. Magn. Magn. Mater.*, vol. 281, pp. 27-35, 2004
- [7] Y. Lee, J. Lee, C.J. Bae, J.-G. Park, H.-J. Noh, J.-H. Park, T. Hyeon. "Large-Scale Synthesis of Uniform and Crystalline Magnetite Nanoparticles Using Reverse Micelles as Nanoreactors under Reflux Conditions," *Adv. Funct. Mater.*, vol. 15, pp. 503-509, 2005
- [8] F.-Y. Cheng, C.-H. Su, Y.-S. Yang, C.-S. Yeh, C.-Y. Tsai, C.-L. Wu, M.-T. Wu, D.-B. Shieh. "Characterization of aqueous dispersions of Fe_3O_4 nanoparticles and their biomedical applications," *Biomaterials*, vol. 26, pp. 729-738, 2005
- [9] F. Caruso, "Colloids and Colloid Assemblies," Wiley-VCH,
- [10] A. Gedanken. "Sonochemistry and its application to nanochemistry," *Current Science*, vol. 85, pp. 1720-1722, 2003
- [11] G.F. Goya, T.S. Berquó, F.C. Fonseca. "Static and dynamic magnetic properties of spherical magnetite nanoparticles," *J. Appl. Phys.*, vol. 94, pp. 3520-3528, 2003